# INTER-NOISE 2006

**3-6 DECEMBER 2006**
**HONOLULU, HAWAII, USA**


# A Landing Gear Noise Reduction Study Based on Computational Simulations


Mehdi R. Khorrami*
NASA LaRC
MS 128
Hampton, VA 23681
USA

David P. Lockard†
NASA LaRC
MS 128
Hampton, VA 23681
USA



## ABSTRACT

Landing gear is one of the more prominent airframe noise sources. Techniques that diminish gear noise and suppress its radiation to the ground are highly desirable. Using a hybrid computational approach, this paper investigates the noise reduction potential of devices added to a simplified main landing gear model without small scale geometric details. The Ffowcs Williams and Hawkings equation is used to predict the noise at far-field observer locations from surface pressure data provided by unsteady CFD calculations. Because of the simplified nature of the model, most of the flow unsteadiness is restricted to low frequencies. The wheels, gear boxes, and oleo appear to be the primary sources of unsteadiness at these frequencies. The addition of fairings around the gear boxes and wheels, and the attachment of a splitter plate on the downstream side of the oleo significantly reduces the noise over a wide range of frequencies, but a dramatic increase in noise is observed at one frequency. The increased flow velocities, a consequence of the more streamlined bodies, appear to generate extra unsteadiness around other parts giving rise to the additional noise. Nonetheless, the calculations demonstrate the capability of the devices to improve overall landing gear noise.


## 1 INTRODUCTION

The past thirty years have seen significant reductions in jet noise through the adoption of high-bypass-ratio turbofan engines on civil aviation transports. Formerly unimportant noise sources such as the airframe have now become a major concern for noise certification and environmental considerations. Airframe noise is most important during aircraft approach and landing, when engines are operating at reduced thrust with high-lift devices and landing gear deployed. Wind tunnel tests[1–3] and fly-over measurements[4] have revealed the leading-edge slats, flap edges, and the landing gear to be the major contributors to airframe noise. Each of the three primary sources of airframe noise are important on different classes of airplanes, but the main landing gear is a dominant source on most modern wide-body transports. Although flow computations of high-lift devices such as flaps and slats received considerable attention in the last decade, the intricacies of a landing gear flow field and its associated sound sources have remained virtually unknown due to overwhelming geometrical complexities. Nonetheless, computational studies of landing gear are beginning to be performed.[5] Souliez *et al.*[6] used an unstructured grid technique to investigate the same baseline landing gear used in this work, but the calculations were restricted to laminar flow with the door removed. The authors previously investigated[7] the baseline gear using a structured grid and the same numerical algorithm employed in the current work. In this paper, we present a computational analysis of noise reduction devices applied to the baseline gear. Our computational approach involves a hybrid strategy. In the first step we perform an unsteady Reynolds Averaged Navier-Stokes (URANS) simulation to provide a near-field solution. Despite continued advances in computational resources and numerical algorithms, it is still prohibitively expensive and often infeasible to attempt to resolve wave propagation from near-field sources to far-field observers. Integral techniques that can predict the far-field signal based solely on near-field input are a means to overcome this difficulty. Hence, the Ffowcs Williams-Hawkings (FW-H) equation[8] solver described by Lockard[9] is used to predict the acoustic


*Email address: m.r.khorrami@nasa.gov
†Email address: d.p.lockard@nasa.gov

signature at various observer locations using surface pressure data from the computational fluid dynamics (CFD) calculation. Additional details can be found in reference 10.

## 2 ACOUSTIC EQUATIONS

The FW-H equation can be written in differential form[11] as

$$\left(\frac{\partial^2}{\partial t^2} - c_o^2 \frac{\partial^2}{\partial x_i \partial x_i}\right)\Big(H(f)\rho'\Big) = \frac{\partial^2}{\partial x_i \partial x_j}\Big(T_{ij}H(f)\Big) - \frac{\partial}{\partial x_i}\Big(F_i\delta(f)\Big) + \frac{\partial}{\partial t}\Big(Q\delta(f)\Big) \tag{1}$$

where

$$T_{ij} = \rho u_i u_j + P_{ij} - c_o^2 \rho' \delta_{ij}, \tag{2}$$

$$F_i = \Big(P_{ij} + \rho u_i (u_j - v_j)\Big)\frac{\partial f}{\partial x_j}, \text{ and} \tag{3}$$

$$Q = \Big(\rho_o v_i + \rho(u_i - v_i)\Big)\frac{\partial f}{\partial x_i}. \tag{4}$$

The dipole term $F_i$ involves an unsteady force, and $Q$ gives rise to a monopole-type contribution that can be thought of as an unsteady mass addition. The function $f = 0$ defines the surface outside of which the solution is desired. The normalization $|\nabla f| = 1$ is used for $f$. The total density and pressure are given by $\rho$ and $p$, respectively. The fluid velocities are $u_i$, while the $v_i$ represent the velocities of the surface $f$. The Kronecker delta, $\delta_{ij}$, is unity for $i = j$ and zero otherwise. The ambient speed of sound is denoted by $c_o$. A prime is used to denote a perturbation quantity relative to the free-stream conditions denoted by the subscript $o$. The Cartesian coordinates and time are $x_i$ and $t$, respectively. The usual convention, which is followed here, involves a quiescent ambient state with $f$ prescribed as a function of time so that it always surrounds a moving source region of interest. $H(f)$ is the Heaviside function which is unity for $f > 0$ and zero for $f < 0$. The derivative of the Heaviside function $H'(f) = \delta(f)$ is the Dirac delta function, which is zero for $f \neq 0$, but yields a finite value when integrated over a region including $f = 0$. The inviscid part, $P_{ij} = p\delta_{ij}$, of the compressive stress tensor $P_{ij}$ is used in this work.

The FW-H equation is an exact rearrangement of the Navier-Stokes equations that allows one to determine the acoustic signal at distant observer locations if the details of the source region are already known. Hence, the Navier-Stokes equations still need to be solved, but only where nonlinear and viscous effects are important. All of the linear propagation can be determined by the FW-H equation. For three-dimensional flows, the time-domain FW-H formulations developed by Farassat[12] are efficient and amenable to numerical computations. Some additional efficiency can be obtained by restricting the source to uniform, rectilinear motion. Furthermore, the equation can be solved in the frequency domain which can be useful if one is only interested in analyzing certain frequencies. The frequency domain solution of FW-H equation can be written in the form[9]

$$H(f)c_o^2\rho'(\mathbf{y},\omega) = -\int_{f=0} F_i(\boldsymbol{\xi},\omega)\frac{\partial G(\mathbf{y};\boldsymbol{\xi})}{\partial y_i}\,ds - \int_{f=0} i\omega Q_n(\boldsymbol{\xi},\omega)G(\mathbf{y};\boldsymbol{\xi})\,ds + I_Q \tag{5}$$

where

$$F_i = \Big(p\delta_{ij} + \rho(u_i - U_i)(u_j + U_j) + \rho_o U_i U_j\Big)\hat{n}_j,$$

$$Q_n = \Big(\rho(u_i + U_i) - \rho_o U_i\Big)\hat{n}_i. \tag{6}$$

The quadrupole term is denoted by $I_Q$ and includes effects such as nonlinear propagation and refraction. In this work, the quadrupole contribution is expected to be small and is neglected. Souliez *et al.*[6] performed

FW-H predictions of landing gear noise using solid and porous integration surfaces and found the solutions to be nearly identical in the far-field, although discrepancies were noted in the near field. The porous surface enclosed a significant region around the gear and should have included most of the quadrupole effects. In this work, our attention is restricted to the far-field where it should be valid to neglect the quadrupole.

## 3 SIMPLIFIED LANDING GEAR MODEL

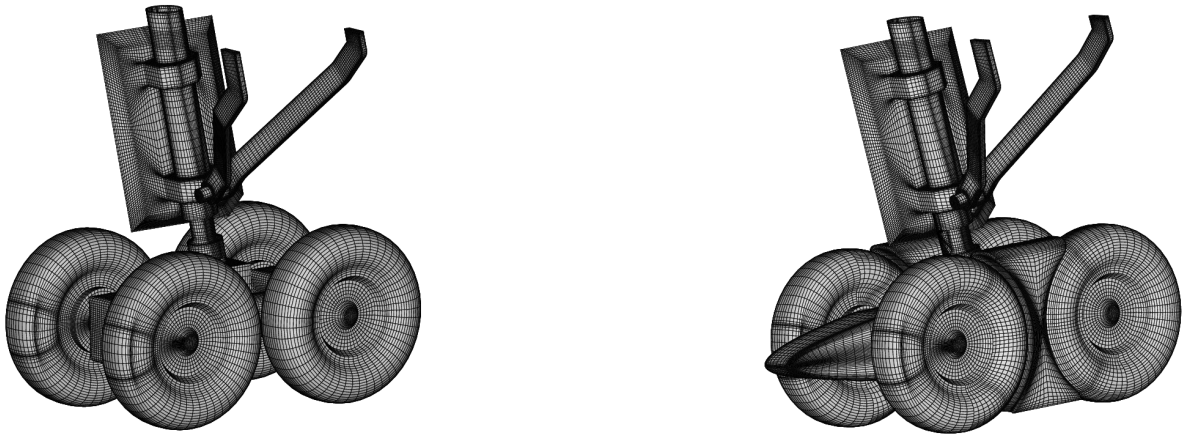

(a) Baseline (b) Modified

Figure 1: Surface grids for a landing gear

Figure 2: Details of landing-gear modifications

The simulated geometry is a four-wheel landing gear model that approximately represents a ten percent scale Boeing 757 main landing gear. The model geometry is fairly complex and composed of four wheels, two side struts, an oleo, a side-door, yokes, a pin, and other structures that join the system together (figure 1 (a)). The gear assembly is mounted on a flat plate that represents the aircraft wing. The baseline structured grid consists of 155 blocks possessing a total of 1.8 million grid points. The modified landing gear in figure 1(b) has 217 blocks and 2.1 million grid points. The modified gear includes fairings around the gear boxes and between the wheels as well as a splitter plate behind the oleo. Figure 2 presents two views of the modified landing gear with some of the components removed so that the added fairings are easily identified. The purpose of the fairings is to smooth the flow around the gear boxes and wheels in order to minimize bluff-body separation zones that are susceptible to large-scale flow oscillations. The splitter plate[13] is supposed to

prevent vortex shedding from the oleo in the region where the door doesn't already disrupt shedding. Figure 1 also shows the grid distribution on the surface of the landing gears. The reference length scale is the gear wheel diameter (3.7in/0.09398 m), and the freestream Mach number is 0.2. The Reynolds number based on the wheel diameter is $1.23 \times 10^6$. The CFD calculation employs the three-dimensional, time-dependent code CFL3D,[14,15] developed at NASA Langley Research Center to solve the three-dimensional, time-dependent, thin-layer Reynolds-Averaged Navier-Stokes (RANS) equations. A more detailed discussion of the CFD calculation can be found in the paper by Li *et al.*[16] The unsteady calculations were run extensively to eliminate all transients. The dimensionless time step based on the wheel diameter was $c_o \Delta t/l = 0.01$.

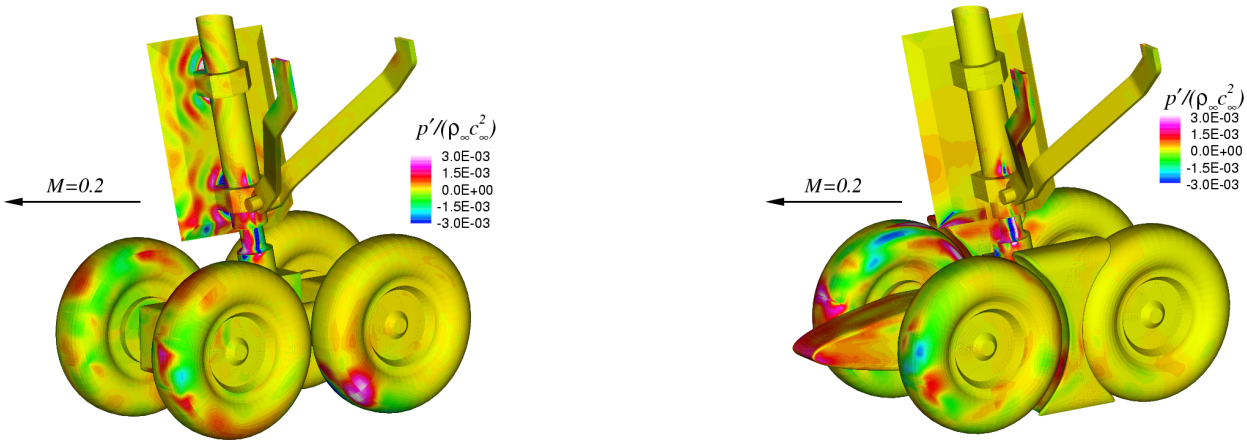


(a) Baseline (b) Modified

Figure 3: Instantaneous perturbation pressure on landing gear.

Contours of the instantaneous perturbation pressure fluctuations on the gear solid surfaces are displayed in figure 3. The surface pressure shows the footprint of the highly nonlinear and complicated interactive near-field flow dynamics. The pressure is nondimensionalized by $\rho_o c_o^2$. Clearly, both the baseline and modified gears have significant pressure fluctuations, but the frequency and peak intensities cannot be inferred from instantaneous quantities. However, the high frequency oscillations on the door of the baseline gear are clearly absent for the modified gear. These waves emanate from small cavities between the door and the upper and lower yokes on the oleo. For the modified gear, these cavities were filled.

## 4 NOISE CALCULATIONS

The noise calculation for the baseline gear involves 181 total subsurfaces comprising the data surface. The modified gear has 224 subsurfaces. All of the subsurfaces are impenetrable, so only the pressure histories are needed. The subsurfaces are a natural consequence of the block structured grid used for the CFD calculation. Each subsurface is a boundary of one of the blocks comprising the grid. Because the problem is so large, the FW-H calculation would have to be performed on subsurfaces regardless of the grid topology. The complete time history record for all subsurfaces requires approximately 14 GB of disk space. Over 12,000 nondimensional time samples with $c_o \Delta t/l = 0.02$ have been collected. Five segments of 4096 samples are used to perform the noise calculations. The results presented in the paper represent an average over the five segments. The segment length corresponds to the time for the flow to pass a wheel sixteen times.

A Ffowcs Williams-Hawkings solver[9] written specifically for airframe noise applications is being used to perform the noise calculations. The calculated sound pressure level spectrum for an observer located directly underneath the gear is presented in figure 4. The observer is located 100 wheel diameters directly beneath the gear. Most of the noise is concentrated at low frequencies because of the absence of the smaller scale

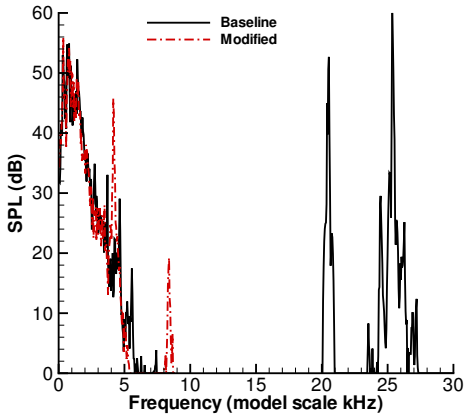


Figure 4: Spectra of the pressure for an observer 100 wheel diameters directly below the gear.

subcomponents in the model and possible excessive diffusion caused by the turbulence model or insufficient grid resolution. However, two high-frequency tones are evident in the signal as shown in figure 4. These tones are those caused by the resonances in the cavities between the yokes and the door. The figure shows that the tone from the upstream cavity is around 20 kHz, and the downstream cavity generates a tone at 26 kHz. There is no evidence of the tones in the modified gear spectra.

### 4.1 SUBSURFACE NOISE PREDICTIONS

Although much of the smaller scale detail is missing from this gear model, the frequency content below 6 kHz is relatively rich and it is not apparent which components are contributing to the different portions of the spectrum. There are several distinct tones that are probably the result of shedding from different components. To investigate the source of the different peaks, the landing gear was divided into 11 regions as show in figure 5. Each region is colored differently to identify each of the subdomains.

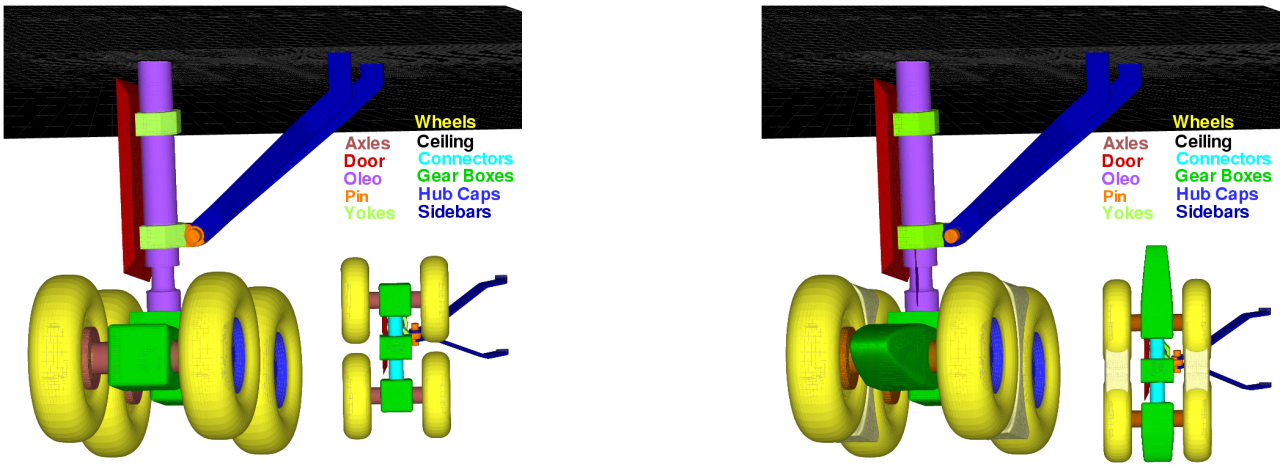


(a) Baseline

(b) Modified

Figure 5: Landing gear colored by component.

The prediction using all of the surfaces (Gear + Ceiling) is compared with the results when using only the ceiling in figure 6. The results are for an observer located 100 wheel diameters directly below the gear. The

results do vary with observer position, but the general trends are similar at most observer locations of interest. The figure shows that for both gears the ceiling accounts for almost all of the noise. The signal from the components is 5-10 dB lower than that of the ceiling. Although one would expect the ceiling to be important because of reflections, it should not be dominant. A calculation without the ceiling where all of the gear components are mirrored still does not produce levels anywhere near those observed with the ceiling alone. Clearly, the ceiling is acting as more than just a reflector as is borne out by figure 7 that shows the instantaneous perturbation pressure contours on the gear and ceiling looking from below. The most intense fluctuations occur on the ceiling in the wake of the sidebars. Although it is likely that the wake from the sidebars would interact with the ceiling, the fluctuations are actually being amplified across and along block boundaries because of insufficient grid resolution. Each of the discontinuities in the contours in figure 7 represents a block interface where extensive patching is used to prevent the propagation of fine resolution to unimportant regions and thus reduce the number of grid points. Because it cannot be determined how much unrealistic amplification is occurring, the prediction when the ceiling is excluded will be used as a reference in the remainder of the paper. The spectra comparison using just the gear components is shown in figure 8. Clearly, the landing gear modifications have produced significant broadband noise reduction, but two additional tones are also apparent. Furthermore, the impact of the modifications on the peak of the spectra has been minimal. A subsurface analysis and source identification will be used to help identify the causes of the tones and the noise reduction.

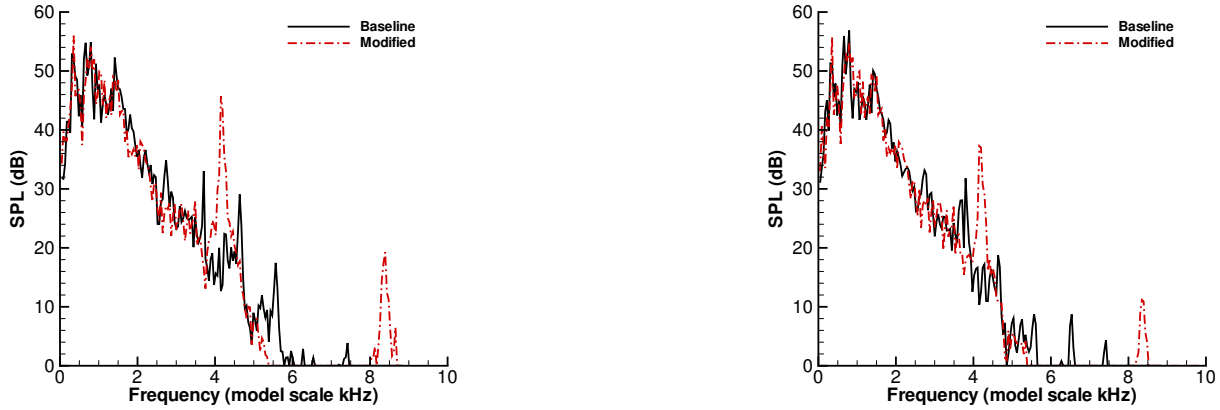


(a) Gear + Ceiling

(b) Ceiling

Figure 6: FW-H results for an observer 100 wheel diameters directly below the landing gear in a $M = 0.2$ flow.

The predicted noise for each of the subsurfaces in figure 5 is shown in figures 9 and 10. The peak levels for the 4.4 kHz tone and its harmonics appear to be associated with the oleo (figure 9(f)). The tones appear in the spectra for the other components because the signal is reflected off the other parts. The tone is associated with unsteadiness in the region around the yoke on the oleo. The tone is also apparent in the baseline spectra at 3.7 kHz. Apparently, streamlining the model accelerated the flow velocity around the oleo increasing the intensity of the unsteadiness and slightly changing the frequency. Although one can detect vortex shedding in this region from the CFD solution, it is asymmetric and associated with a complex interaction of the flow around the oleo, yoke, and door. The splitter plate appears effective at eliminating normal Strouhal shedding which is expected around 1 kHz for the contracted region of the oleo where the flow is not disrupted by the door. The 1 kHz tone observed for the baseline model is virtually eliminated by the splitter plate.

The broadband shape of the gear spectra is generated by the gear boxes (9(c)), the connectors between the gear boxes (9(d)), and the wheels (10(c)). Significant broadband reduction is apparent for all three components on the modified gear. However, the reduction below 500 Hz is negligible, so the overall peak of the noise is unchanged.

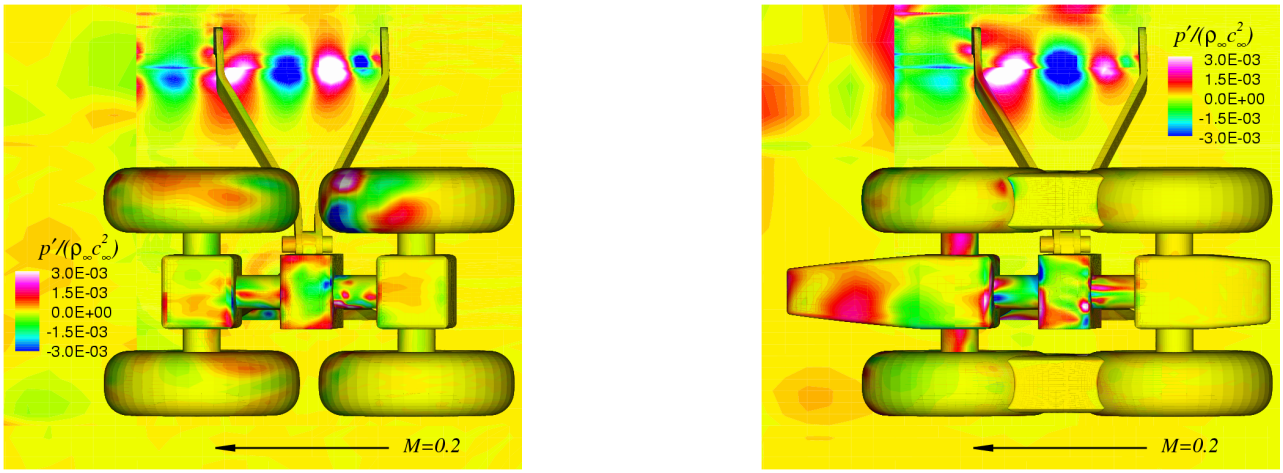


(a) Baseline (b) Modified

Figure 7: Instantaneous perturbation pressure on the landing gear.

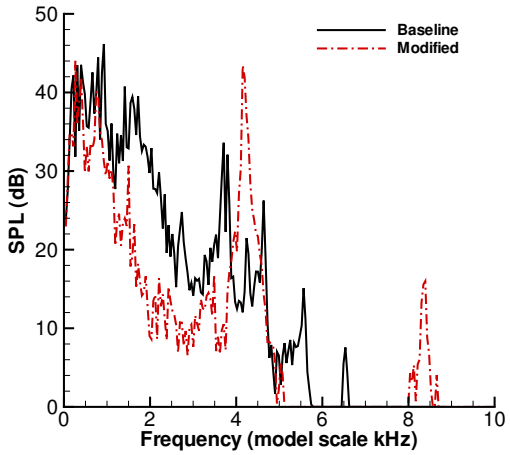


Figure 8: FW-H results for an observer 100 wheel diameters directly below the landing gear in a $M = 0.2$ flow. Only the gear components are used to make the prediction.

Noise reduction is also observable in the spectra for the axles (9(a)), door (9(b)), pin (10(a)), and yokes (10(d)). In some cases, the observed reduction is primarily a result of reducing sources on other components whose footprint extends to other areas. Nonetheless, the general trend of reduced noise is encouraging. The spectra for the sidebars (10(b)) is relatively unchanged by any of the modifications which is expected because they are unchanged from the baseline configuration. However, the spectra for the hub caps (9(e)) actually increased, presumably because of accelerated flow around the wheels caused by the additional streamlined parts.

## 5 RESOLUTION AND TURBULENCE MODEL

The spectra obtained from the simulations is restricted to low frequencies which makes it difficult to assess the total effect of the noise reduction devices. The model is approximately $10\%$ of full scale, so full scale frequencies up to 600 Hz have been obtained from the simulations. Measurements of landing gear noise typically extend to several kHz. One possible cause of the loss of the high frequency content is the mesh. It is difficult to maintain adequate resolution throughout the flowfield while still making the problem tractable. Furthermore, excessive patching is required for a complex geometry such as a landing gear, and errors at block interfaces are apparent in the solution. However, a calculation on a finer grid has failed to completely fill out the spectra. Another possible source of error is the turbulence model. We have used an unsteady RANS calculation with a $k-\omega$ turbulence model tuned for steady flow. Although qualitatively good results have been obtained with this approach for unsteady problems, it is well known that the turbulence model is overly dissipative. We have also run the landing gear problem as a detached-eddy simulation[17] (DES) as proposed by Spalart. The DES model essentially reduces the level of eddy viscosity in regions away from solid surfaces when the grid is sufficiently fine. The comparison of the spectra in figure 11 shows that the DES solution does have frequency content out to 9 kHz, and the levels are significantly higher above 2 kHz. Although a significant improvement, the levels are still lower than expected based on experiment.

## 6 CONCLUSIONS

The current investigation has validated the noise reduction potential of fairings around the wheels and gear boxes of a landing gear, as well as the potential elimination of vortex shedding behind cylindrical bodies by the addition of a splitter plate in the wake. Although significant broadband noise reduction was obtained, the peak of the spectrum was unchanged. Furthermore, the level of a tone was significantly increased. The tone was affected because the flow around certain components was accelerated by the streamlining of some of the bluff bodies comprising the gear. Hence, one should be aware that there can be unexpected consequences of the addition of noise reduction devices. Two high frequency tones associated with unsteadiness in small cavities between the yokes and the door were eliminated by filling the cavities. Small cavities should be avoided when possible because of the potential for resonances in these regions.

The accuracy of the simulations was examined through grid refinement and changing the turbulence model. A finer mesh only resulted in minor changes to the calculation, but a DES simulation did improve the range of resolved frequencies. However, there is still a large discrepancy with what is observed in experiments. Nonetheless, it is expected that the effect of noise reduction devices investigated in this work are most influential in the range of frequencies resolved by the current calculations, so the most important aspects of the physics have been captured.

## REFERENCES

[1] Choudhari, M. M., Lockard, D. P., Macaraeg, M. G., Singer, B. A., Streett, C. L., Neubert, G. R., Stoker, R. W., Underbrink, J. R., Berkman, M. E., Khorrami, M. R., and Sadowski, S. S., "Aeroacoustic Experiments in the Langley Low-Turbulence Pressure Tunnel," *NASA TM 2002-211432*, 2002.

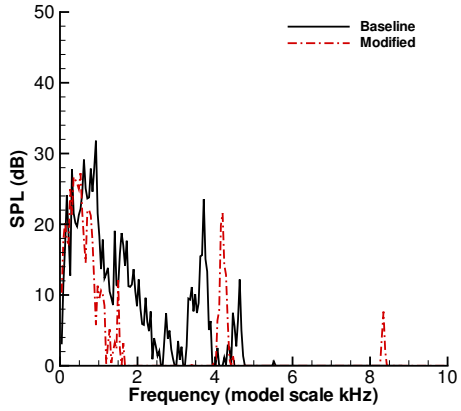


(a) Axles

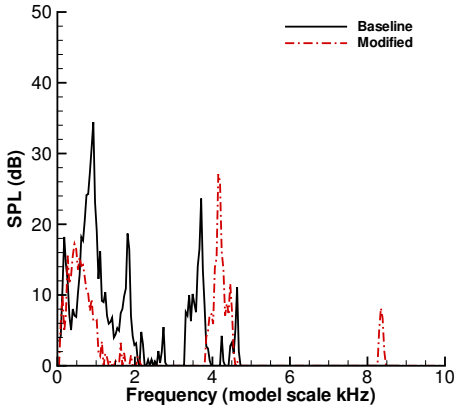


(b) Door

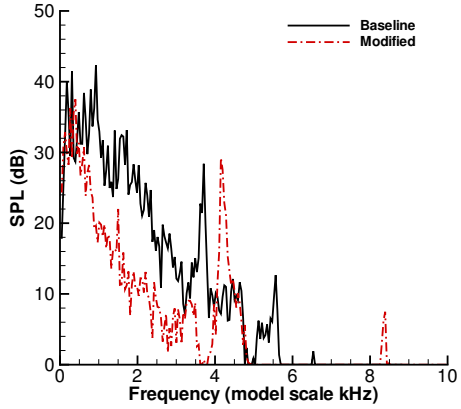


(c) Gear Boxes

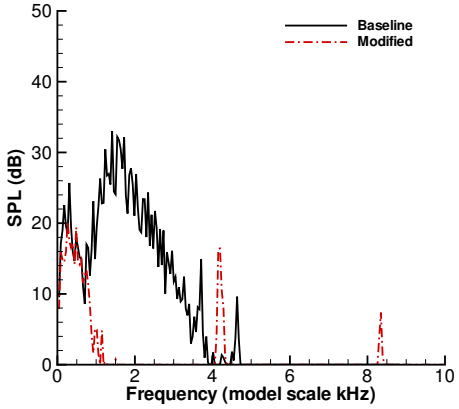


(d) Gear Box Connectors

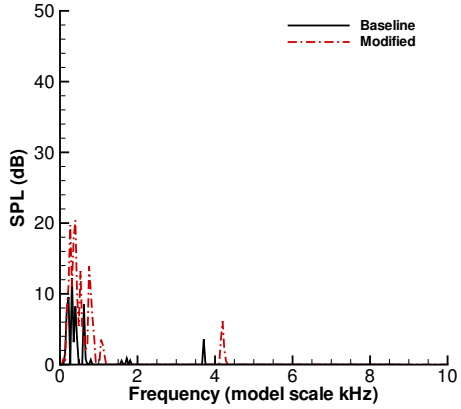


(e) Hub Caps

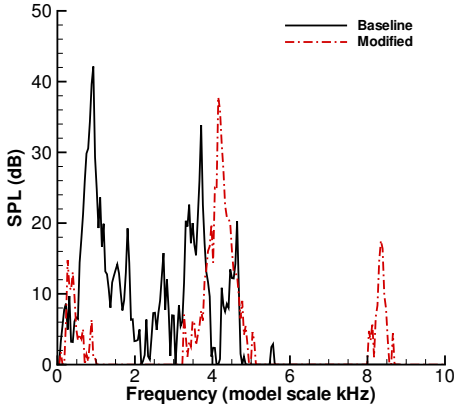


(f) Oleo

Figure 9: Noise contributions for an observer 100 wheel diameters directly below the landing gear in a $M = 0.2$ flow.

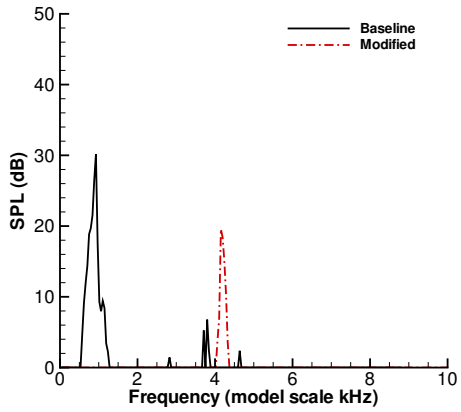


(a) Pin

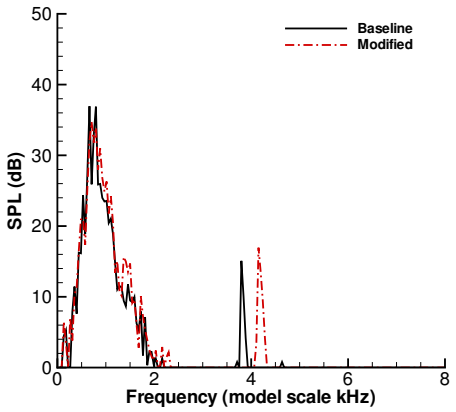


(b) Sidebars

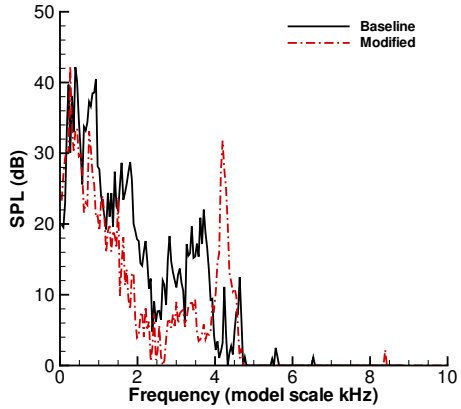


(c) Wheels

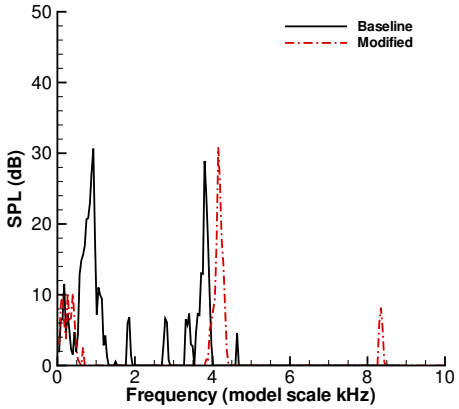


(d) Yokes

Figure 10: Noise contributions for an observer 100 wheel diameters directly below the landing gear in a $M = 0.2$ flow.

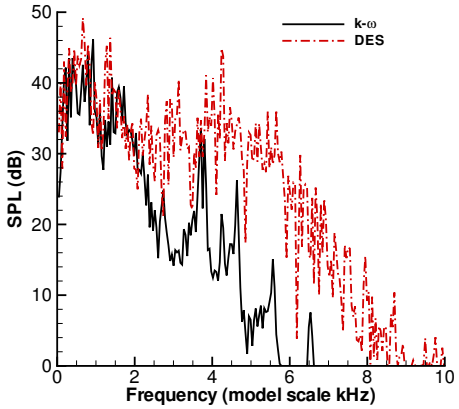


Figure 11: Spectra comparison for an observer located 100 wheel diameters directly below the gear in a $M = 0.2$ flow.

[2] Streett, C. L., Lockard, D. P., Khorrami, M. R., and Choudhari, M., "In Search of the Physics - The Interplay of Experiment and Computation in Airframe Noise Research; Flap-edge Noise," AIAA-03-0979, Presented at the 41st AIAA Aerospace Sciences Meeting & Exhibit, Reno, NV, 2003.

[3] Khorrami, M. R., Choudhari, M., Singer, B. A., Lockard, D. P., and Streett, C. L., "In Search of the Physics - The Interplay of Experiment and Computation in Slat Aeroacoustics," AIAA-03-0980, Presented at the 41st AIAA Aerospace Sciences Meeting & Exhibit, Reno, NV, 2003.

[4] Stoker, R., Guo, Y., Streett, C., and Burnside, N., "Airframe Noise Source Locations of a 777 Aircraft in Flight and Comparisons with Past Model-Scale Tests," AIAA-03-3111, Presented at the 9th AIAA/CEAS Aeroacoustics Conference and Exhibit in Hilton Head, SC, 2003.

[5] Hedges, L. S., Travin, A. K., and Spalart, P. R., "Detached-Eddy Simulations Over a Simplified Landing Gear," *Journal of Fluids Engineering*, Vol. 124, 2002, pp. 413–423.

[6] Souliez, F. J., Long, L. N., Morris, P. J., and Sharma, A., "Landing Gear Aerodynamic Noise Prediction Using Unstructured Grids," *International Journal of Aeroacoustics*, Vol. 1, No. 2, 2002, pp. 115–135.

[7] Lockard, D. P., Khorrami, M. R., and Li, F., "Aeroacoustic Analysis of a Simplified Landing Gear," AIAA-03-3111, Presented at the 9th AIAA/CEAS Aeroacoustics Conference and Exhibit in Hilton Head, SC, 2003.

[8] Ffowcs Williams, J. E. and Hawkings, D. L., "Sound generation by turbulence and surfaces in arbitrary motion," *Philosophical Transactions of the Royal Society of London A*, Vol. 342, 1969, pp. 264–321.

[9] Lockard, D., "A Comparison of Ffowcs Williams-Hawkings Solvers for Airframe Noise Applications," AIAA Paper 2002-2580, 8th AIAA/CEAS Aeroacoustics Conference, Breckenridge, CO, June 17–19, 2002.

[10] Lockard, D. P. and Khorrami, M. R., "Computational Analysis of Landing Gear Noise Reduction," CDTM 10043, NASA, May 2004.

[11] Crighton, D. G., Dowling, A. P., Ffowcs Williams, J. E., Heckl, M., and Leppington, F. G., *Modern Methods in Analytical Acoustics*, chap. 11, Springer-Verlag, London, 1992, pp. 334–342.

[12] Farassat, F., "Linear Acoustic Formulas for Calculation of Rotating Blade Noise," *AIAA Journal*, Vol. 19, No. 9, 1981, pp. 1122–1120.

[13] Apelt, C. J., West, G. S., and Szewzyk, A. A., "The Effect of Wake Splitter Plates on the Flow Past Circular Cylinders in the Range $10 < Re < 5 \times 10^4$," *Journal of Fluid Mechanics*, Vol. 61, No. 1, 1970, pp. 187–198.

[14] Rumsey, C., Biedron, R., and Thomas, J., "CFL3D: Its History and Some Recent Applications," TM 112861, NASA, May 1997, presented at the Godonov's Method for Gas Dynamics Symposium, Ann Arbor, MI.

[15] Krist, S. L., Biedron, R. T., and Rumsey, C., "CFL3D User's Manual (Version 5)," NASA/TM-1998-208444, 1998.

[16] Li, F., Khorrami, M. R., and Malik, M. R., "Unsteady Simulations of a Landing-Gear Flow Field," AIAA Paper 2002-2411, 8th AIAA/CEAS Aeroacoustics Conference, Breckenridge, CO, June 17–19, 2002.

[17] Squires, K. D., Forsythe, J. R., Morton, S. A., Strang, W. Z., Wurtzler, K. E., Tomaro, R. F., Grismer, M. J., and Spalart, P. R., "Progress on Detached-Eddy Simulation of Massively Separated Flows," AIAA-02-1021, Presented at the 40th AIAA Aerospace Sciences Meeting and Exhibit in Reno, NV, 2002.